Photonic crystal heterostructures: Waveguiding phenomena and methods of solution in an envelope function picture

Mathieu Charbonneau-Lefort, Emanuel Istrate, Mathieu Allard, Joyce Poon, and Edward H. Sargent

Department of Electrical and Computer Engineering, University of Toronto, 10 King's College Road, Toronto, Canada, M5S 3G4

We present an envelope approximation formalism to study three-dimensional photonic crystal heterostructures which only requires knowledge of the bulk crystal band structure and heterostructure design. Applying this method to photonic crystal waveguides, we predict within 1% accuracy the frequencies of guided modes and obtain the correct waveguided mode shapes. We show that guided modes are allowed for wave vectors where the curvature of a band in a direction perpendicular to the plane of the waveguide has the same sign as the refractive index contrast between the core and the cladding. We show that elementary waveguide theory can be employed to compute mode shapes and dispersion relations.

I. INTRODUCTION

Photonic crystals have been the subject of intense theoretical work over the past decade, marked by the development of plane-wave techniques adapted to periodic structures,[1] transfer matrix methods,[2] and different types of numerical schemes to solve Maxwell's equations.[3] The computation of the band structure of photonic crystals is now a well-established process, both in two- and three-dimensional structures.

Just like homogeneous bulk electronic crystals, photonic crystals on their own are of limited use. It has been proposed to take advantage of their unique properties by introducing defects to make waveguides,[4–6] bends,[7] branches,[8] and filters.[9] When the length scale of these defects is substantially greater than the lattice constant, we call them *heterostructures* by analogy with semiconductor devices made by the assembly of different types of crystals.

Whereas computations on bulk crystals can be carried out using well-known techniques, the theoretical study of heterostructures and other defects represents a significant computational challenge. The fully vectorial solution of Maxwell's equations on a nonperiodic structure is memory and time intensive. For this reason, most work to date has been focused on two-dimensional (2D) structures.

In the present work, we investigate photonic crystal heterostructures using an envelope formalism. Our method focuses on the envelope of the modes while accounting for the essential consequences of the crystalline structure of the constituents of the heterostructure. This approach allows us to investigate 3D crystals and provides a physical picture of the behavior of light inside the superstructure. To demonstrate this, we employ our method to study photonic crystal waveguides, showing how waveguiding in photonic crystals can be explained in analogy with available formalism used in analyzing dielectric waveguides. We show that the quantitative results obtained using the envelope formalism are in excellent agreement with a fully fledged computation of the modes in photonic crystal waveguides.

Our approach is inspired by the formalism developed by Slater[10] in 1949 to explain the motion of electrons in perturbed periodic lattices. By applying the results of Wannier,[11] Slater showed that in the presence of a slowly varying perturbation of the lattice δV, the envelope $\Psi(\mathbf{r})$ of the electron wave function obeys the Schrödinger-like equation

$$[E_0(-i\hbar\nabla) + \delta V(\mathbf{r})]\Psi(\mathbf{r}) = E\Psi(\mathbf{r}), \qquad (1)$$

where E is the energy of the electron and $E_0(-i\hbar\nabla)$ is the operator obtained from the energy $E_0(\mathbf{p})$ of an electron in an unperturbed lattice by replacing the momentum components by their associated derivative operators. This work laid the foundation of the effective-mass theory used in the 1950's to calculate the energy states of donors and acceptors in semiconductors.[12–14]

In semiconductor physics, both small-scale defects such as impurities, and large-scale perturbations such as heterojunctions, are required to build useful devices. The investigation of each type of defect requires its own theoretical apparatus. In the case of photonic crystals, states localized by small-scale defects have been addressed recently[15] using concepts derived from Wannier's theory. In this work, we provide a way of studying heterostructures, whose dimensions are substantially larger than the crystal dimensions. We show that in these circumstances the envelope of the electromagnetic field obeys an equation similar to Eq. (1). This will allow us to provide a rigorous derivation of the intuitive idea behind the envelope approximation formalism depicted in Fig. 1: once the dispersion relations of the constituent materials arising from crystal-length-scale features are obtained, these may then be used as effective-medium inputs to the solution of the heterostructure in the slowly varying envelope picture.

II. ENVELOPE APPROXIMATION FORMALISM

In bulk photonic crystals defined by the periodic dielectric constant $\epsilon(\mathbf{r})$, the electric field modes $\mathbf{E}_{n\mathbf{k}}$ with frequencies ω_n satisfy the wave equation

$$\vec{\nabla}\times(\vec{\nabla}\times\mathbf{E}_{n\mathbf{k}}(\mathbf{r})) = \frac{\omega_n^2}{c^2}\epsilon(\mathbf{r})\mathbf{E}_{n\mathbf{k}}(\mathbf{r}). \qquad (2)$$
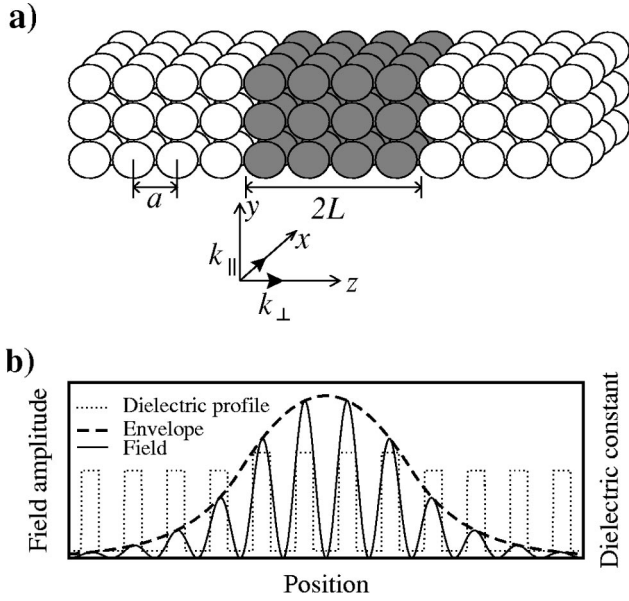
a)

b)

FIG. 1. (a) 3D photonic crystal slab waveguide. (b) Intuitive picture behind the envelope approximation formalism: the fast-varying features of the electromagnetic field are due to the crystal while its envelope is determined by the shape of the heterostructure.

By the Bloch-Floquet theorem, the modes take the form

$$\mathbf{E}_{n\mathbf{k}}(\mathbf{r}) = \mathbf{u}_{n\mathbf{k}}(\mathbf{r})e^{i\mathbf{k}\cdot\mathbf{r}}, \tag{3}$$

where the Bloch functions $\mathbf{u}_{n\mathbf{k}}$ have the periodicity of the lattice. As discussed in Ref. 16, the electric field modes are orthogonal to one another with respect to the dielectric constant

$$\int \mathbf{E}_{n'\mathbf{k}'}^{*}(\mathbf{r}) \cdot \epsilon(\mathbf{r})\mathbf{E}_{n\mathbf{k}}(\mathbf{r})d\mathbf{r} = \delta_{nn'}\delta(\mathbf{k}-\mathbf{k}'). \tag{4}$$

Similarly, the Bloch functions are normalized over a unit cell of volume V_0 so that

$$\frac{1}{V_0}\int_{\text{cell}} \mathbf{u}_{n'\mathbf{k}}^{*}(\mathbf{r}) \cdot \epsilon(\mathbf{r})\mathbf{u}_{n\mathbf{k}}(\mathbf{r})d\mathbf{r} = (2\pi)^3\delta_{nn'}. \tag{5}$$

In this paper, we consider heterostructures defined by a spatially varying perturbation $\Delta(\mathbf{r})$ modulating the dielectric constant of the bulk crystal. This modulation varies slowly over a unit cell, which supposes that the length scale of the perturbation is large compared to the lattice constant. The wave equation becomes

$$\vec{\nabla}\times(\vec{\nabla}\times\mathbf{E}_{\lambda}(\mathbf{r})) = \frac{\omega_{\lambda}^2}{c^2}\epsilon(\mathbf{r})[1+\Delta(\mathbf{r})]\mathbf{E}_{\lambda}(\mathbf{r}). \tag{6}$$

Throughout this derivation, the subscript λ refers to perturbed quantities. We expand the perturbed mode $\mathbf{E}_{\lambda}$ using the basis of the unperturbed modes

$$\mathbf{E}_{\lambda}(\mathbf{r}) = \sum_n \int W_n(\mathbf{k})\mathbf{E}_{n\mathbf{k}}(\mathbf{r})d\mathbf{k}, \tag{7}$$

where $W_n(\mathbf{k})$ are unknown functions defining the expansion of the mode in k space. Substituting into the wave equation (6) and making use of our knowledge of the unperturbed modes Eq. (2), we obtain

$$\sum_n \int W_n(\mathbf{k})\omega_n^2(\mathbf{k})\epsilon(\mathbf{r})\mathbf{E}_{n\mathbf{k}}(\mathbf{r})d\mathbf{k}$$

$$= \sum_n \int W_n(\mathbf{k})\omega_{\lambda}^2\epsilon(\mathbf{r})[1+\Delta(\mathbf{r})]\mathbf{E}_{n\mathbf{k}}(\mathbf{r})d\mathbf{k}. \tag{8}$$

We take the inner product between every member of this equation and a mode $\mathbf{E}_{n'\mathbf{k}'}$, that is, we multiply by $\mathbf{E}_{n'\mathbf{k}'}^{*}$ and integrate over the entire crystal. By orthogonality of modes, the leftmost term becomes

$$W_{n'}(\mathbf{k}')\omega_{n'}^2(\mathbf{k}'). \tag{9}$$

The first right-hand-side term is treated in a similar fashion. To evaluate the term containing the perturbation, we make two approximations. First, we assume that the perturbation varies over a length scale that is much larger than the crystal periodicity. As explained in detail in the appendix, assuming that the Fourier coefficients of $\Delta(\mathbf{r})$ take large values for $|k| \ll 1/a$ allows us to neglect all but the first term in the Fourier series of $\mathbf{u}_{n'\mathbf{k}'}^{*} \cdot \epsilon(\mathbf{r})\mathbf{u}_{n\mathbf{k}}$. Second, we assume that two Bloch modes $\mathbf{u}_{n'\mathbf{k}'}$ and $\mathbf{u}_{n\mathbf{k}}$ associated with different bands are orthogonal to one another even though they are not taken at the same wave vector. This obviates summation over all bands—thus it entails that the perturbation causes negligible coupling between bands. Therefore (see the Appendix), the perturbation (rightmost) term of Eq. (8) becomes

$$(2\pi)^3\omega_{\lambda}^2\int \Delta(\mathbf{r})e^{-i\mathbf{k}'\cdot\mathbf{r}}\left[\int W_{n'}(\mathbf{k})e^{i\mathbf{k}\cdot\mathbf{r}}d\mathbf{k}\right]d\mathbf{r}. \tag{10}$$

We define $F_n(\mathbf{r})$, the Fourier transform of $W_n(\mathbf{k})$:

$$F_n(\mathbf{r}) \equiv \int W_n(\mathbf{k})e^{i\mathbf{k}\cdot\mathbf{r}}d\mathbf{k}. \tag{11}$$

We show later in this work that F_n is the envelope function of the mode.

The term (10) contains the inverse Fourier transform of the product $\Delta(\mathbf{r})F_{n'}(\mathbf{r})$. Taking the Fourier transform of the projection of Eq. (8) along $\mathbf{E}_{n'\mathbf{k}'}$ and dropping the primes, we obtain the equation describing the behavior of the envelope of the mode of the heterostructure:

$$\omega_n^2(-i\vec{\nabla})F_n(\mathbf{r}) = \omega_{\lambda}^2[1+\Delta(\mathbf{r})]F_n(\mathbf{r}), \tag{12}$$

where $\omega_n^2(-i\vec{\nabla})$ is the operator obtained from $\omega_n^2(\mathbf{k})$ by replacing the wavevector components k_x, k_y, and k_z by the derivatives $-i\partial/\partial x$, $-i\partial/\partial y$ and $-i\partial/\partial z$. Throughout this paper, we refer to Eq. (12) as the *envelope equation*.

III. INTERPRETATION OF THE ENVELOPE EQUATION

The envelope approximation formalism provides a very simple way of investigating photonic crystal heterostructures. A scalar envelope equation replaces the full vectorial

wave equation, and so it may be possible to obtain analytic expressions for the frequency and envelope of the heterostructure modes. The method applies to any type of photonic crystal: only knowledge of its band structure is required, through the operator $\omega_n^2(-i\vec{\nabla})$. Therefore, once the crystal has been characterized by other methods, be they computational or experimental, the simulation of heterostructures follows easily

The treatment used in deriving Eq. (12) requires that the length scale of the heterostructure be significantly larger than that of the crystal. The crystalline structure (i.e., periodicity and Bravais lattice) must be the same everywhere in the heterostructure for Floquet's theorem to hold. The heterostructure profile must be described by a multiplication by a factor $1+\Delta(\mathbf{r})$. This description of the heterostructure simplifies considerably the mathematical treatment of the problem and places emphasis on the role of expanding/contracting dispersion relations along the energy axis, as we shall see in Sec. V. It describes photonic crystal heterostructures consisting entirely of photonic crystals. To treat a more general class of heterostructures, including air-photonic crystal waveguides, the envelope equation is required to hold in every region of the heterostructure separately. In this case, the envelope function is piecewise defined and the different regions can be joined by satisfying the boundary conditions (continuity of the envelope function and of its derivative). This approach is similar to that employed in semiconductor physics, where every semiconductor forming the heterostructure is described by a characteristic effective mass.

In deriving the envelope equation, we assumed that the perturbation did not cause significant coupling between the bands. This allowed us to simplify the projection of the rightmost term of Eq. (8) on a mode of the bulk crystal, leading to expression (10). This assumption is an excellent one for small perturbations. We note that the constituent rapidly varying media may be high-contrast photonic bandgap materials, at no expense to the validity of solution. It is only the slowly varying heterostructure which is considered perturbatively in the present treatment, and which is subject to the limitations of requirement of a modest perturbation.

We conclude this discussion by showing that the functions $F_n(\mathbf{r})$ are the envelope functions of the heterostructure modes. While it is necessary to solve Eq. (12) for every band, these equations are not independent because they share the eigenvalue ω_λ. Since it is possible to satisfy only one of these at a time, there exists one perturbed state for every band. We drop the summation over all bands in Eq. (7) and denote $\mathbf{E}_{\lambda n}=\int W_n \mathbf{E}_{n\mathbf{k}} d\mathbf{k}$ the heterostructure mode having the frequency $\omega_{\lambda n}$ associated with band n. The operator $\omega_n^2(-i\vec{\nabla})$ can be expanded in the vicinity of the wave vector $\mathbf{k}_0$ of the light in the crystal:

$$\omega_n^2(-i\vec{\nabla})=\omega_n^2(\mathbf{k}_0)+\sum_{\xi=x,y,z}\left.\frac{\partial\omega_n^2}{\partial k_\xi}\right|_{\mathbf{k}_0}\left(\frac{1}{i}\frac{\partial}{\partial k_\xi}-k_{0\xi}\right)+\cdots.$$

$$(13)$$

This suggests a solution of the envelope equation of the form

$$F_{n\mathbf{k}_0}(\mathbf{r})=e^{i\mathbf{k}_0\cdot\mathbf{r}}f_{n\mathbf{k}_0}(\mathbf{r}). \qquad (14)$$

By Eqs. (3), (7), (11), and (14), the modes may be written

$$\mathbf{E}_{\lambda n\mathbf{k}_0}(\mathbf{r})=\int \widetilde{f}_{n\mathbf{k}_0}(\mathbf{k}-\mathbf{k}_0)\mathbf{u}_{n\mathbf{k}}(\mathbf{r})e^{i\mathbf{k}\cdot\mathbf{r}}d\mathbf{k}, \qquad (15)$$

where $\widetilde{f}_{n\mathbf{k}_0}(\mathbf{k})$ denotes the inverse Fourier transform of $f_{n\mathbf{k}_0}(\mathbf{r})$. Because the function $f_{n\mathbf{k}_0}(\mathbf{r})$ varies over the same length scale as $\Delta(\mathbf{r})$, as can be seen by substituting Eq. (14) into (12), its Fourier components $\widetilde{f}_n(\mathbf{k}-\mathbf{k}_0)$ take large values for $\mathbf{k}\approx\mathbf{k}_0$ only. Assuming that $\mathbf{u}_{n\mathbf{k}}(\mathbf{r})\approx\mathbf{u}_{n\mathbf{k}_0}(\mathbf{r})$ over this range, we remove $\mathbf{u}_{n\mathbf{k}_0}(\mathbf{r})$ from the integral to obtain

$$\mathbf{E}_{\lambda n\mathbf{k}_0}(\mathbf{r})=F_{n\mathbf{k}_0}(\mathbf{r})\mathbf{u}_{n\mathbf{k}_0}(\mathbf{r})=f_{n\mathbf{k}_0}(\mathbf{r})\mathbf{E}_{n\mathbf{k}_0}(\mathbf{r}). \qquad (16)$$

The physical meaning of the envelope functions $F_{n\mathbf{k}_0}$ is now clear: they modulate the bulk crystal Bloch functions. This result confirms the validity of the intuitive physical picture presented in Fig. 1: at the crystalline length scale, the field keeps features similar to that of the bulk material, but its envelope is determined by the heterostructure.

IV. PHOTONIC CRYSTAL WAVEGUIDES

We now solve the photonic crystal waveguide problem using the envelope approximation method. We show that the dispersion relation, shapes and number of modes and single-mode condition are obtained by a treatment similar to that of usual dielectric waveguides.

We consider a slab waveguide parallel to the x-y plane, the z axis being perpendicular to the plane of the guide, as shown in Fig. 1(a). We define the components of the wave vector in the propagation direction $k_\parallel$ and in the transverse direction $k_\perp$.

The waveguide is regarded as a perturbation from the bulk crystal. For a guide of width $2L$ and dielectric contrast Δ_0, the perturbation is defined as

$$\Delta(z)=\begin{cases} \Delta_0 & \text{if } |z|<L, \\ 0 & \text{if } |z|>L. \end{cases} \qquad (17)$$

Because of the assumptions of the envelope approximation method, the core and the cladding must have the same Bravais lattice and periodicity.

Since the perturbation is a function of z only, the envelope function solution must depend on z only. Due to the symmetry of the waveguide, the derivatives appearing in the envelope equation must be of even order. The wave vector $\mathbf{k}_0$ must correspond to an extremum of the band structure in the transverse ($k_\perp$ or k_z) direction, which ensures that $\partial\omega_n^2(\mathbf{k}_0)/\partial k_z=0$.

If terms are kept up to second order in the Taylor expansion (13), and using Eq. (14), the envelope equation (12) becomes

$$\frac{1}{2m_\perp} \frac{d^2 f_{n\mathbf{k}_0}(z)}{dz^2} = [\omega_n^2(\mathbf{k}_0) - \omega_\lambda^2[1 + \Delta(z)]] f_{n\mathbf{k}_0}(z),$$

$$(18)$$

where, by analogy with quantum mechanics, we define

$$\frac{1}{m_\perp} \equiv \frac{\partial^2 \omega_n^2(\mathbf{k}_0)}{\partial k_z^2},$$

$$(19)$$

an effective-mass-like term describing the curvature of the band. Although we assume that the bands are well approximated by a quadratic expansion, this does not have to be the case for the general method developed herein to apply: higher-order terms could be retained at the expense of increased complexity. The solution of Eq. (18) is

$$f_{n\mathbf{k}_0}(z) = \begin{cases} A\cos(Kz) & \text{for } |z| < L \quad \text{(even modes)}, \\ B\sin(Kz) & \text{for } |z| < L \quad \text{(odd modes)}, \\ Ce^{-\gamma|z|} & \text{for } |z| > L \end{cases}$$

$$(20)$$

with

$$K \equiv \sqrt{2m_\perp[\omega_{\lambda n}^2(1+\Delta_0) - \omega_n^2(\mathbf{k}_0)]} \qquad (21)$$

and

$$\gamma \equiv \sqrt{2m_\perp[\omega_n^2(\mathbf{k}_0) - \omega_{\lambda n}^2]}. \qquad (22)$$

The frequency can be eliminated to give the equation of an ellipse

$$\frac{u^2}{U^2} + \frac{v^2}{V^2} = 1, \qquad (23)$$

where

$$u \equiv KL, \quad U^2 \equiv 2m_\perp \omega_n^2(\mathbf{k}_0)\Delta_0 L^2 \qquad (24)$$

and

$$v \equiv \gamma L, \quad V^2 \equiv \frac{2m_\perp \omega_n^2(\mathbf{k}_0)\Delta_0 L^2}{1+\Delta_0}. \qquad (25)$$

Enforcing the continuity of the solution and of its derivative at the interface $z = \pm L$ gives an additional equation

$$v = u\tan(u) \qquad (26)$$

for the even modes or

$$v = u\tan(u - \pi/2) \qquad (27)$$

for the odd modes.

In summary, the guided modes are given by the intersection of two curves: the ellipse (23) and one of the functions (26) or (27). There exists at least one even mode. The single-mode condition is given by $U < \pi/2$, or

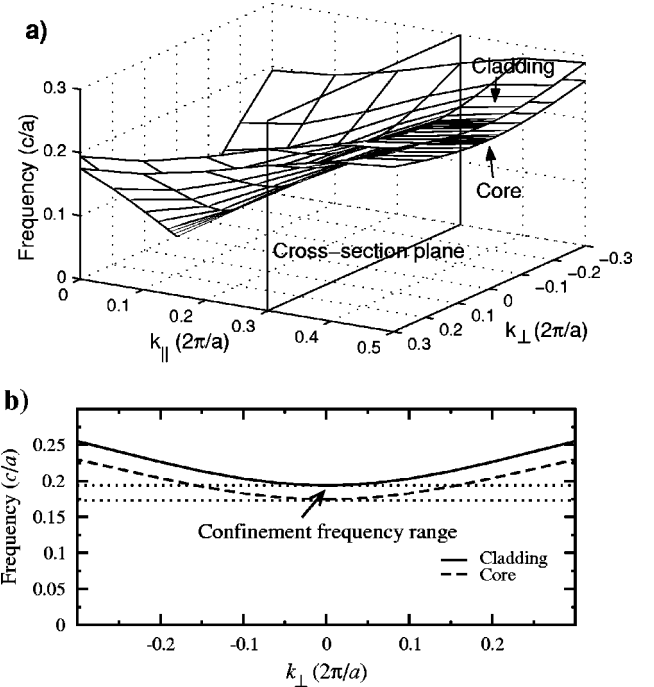$$8m_\perp \omega_n^2(\mathbf{k}_0)\Delta_0 L^2 < \pi^2. \qquad (28)$$

FIG. 2. Photonic crystal waveguiding: guided modes exist in a range of frequencies corresponding to an allowed band in the core but not in the cladding. (a) First band in the cladding and core materials for a contrast of $\Delta_0 \approx 0.25$. (b) Cross section of the band at $k_\parallel = 0.3(2\pi/a)$ showing the confinement frequency range.

V. DISCUSSION

The formalism employed to find the number and frequency of guided modes and the single-mode condition is similar to that encountered in the study of slab dielectric waveguides. The major difference is the effective-mass-like term which controls the size of the ellipse and affects the number of allowed modes. Since the band structure is usually anisotropic, the guiding properties depend on the orientation of the waveguide with respect to the crystal. The transverse band structure curvature is an additional parameter that can be engineered to achieve desired waveguiding properties such as modal group velocity or dispersion.

In deriving these results, no assumption has been made regarding the dielectric contrast Δ_0 between the core and the cladding. As such, guided modes can exist even though the average refractive index in the core is lower than that of the cladding (i.e., $\Delta_0 < 0$), provided $m_\perp$ is negative too. The envelope approximation formalism allows us to state this important conclusion: photonic crystal waveguiding is possible for wave vectors where the curvature of the band in the transverse direction has the same sign as the dielectric contrast between the core and the cladding.

Figure 2 illustrates the mechanism of photonic crystal waveguiding assuming that the contrast Δ_0 and the transverse curvature of the band are both positive. The band structure in the core is compressed vertically by a factor of $\sqrt{1+\Delta_0}$ compared to that of the cladding. This creates a frequency range where light is allowed to propagate in the core but not in the cladding. A full bandgap in the cladding material is therefore not required to achieve waveguiding.

The analogous mechanism applies when Δ_0 and the curvature of the band are both negative.

VI. QUANTITATIVE RESULTS

We have analyzed a slab waveguide using the envelope formalism developed herein. We consider 2D photonic crystals to enable full quantitative comparison of envelope function results with exact numerical results. 3D crystals represent a particularly powerful application of the envelope function formalism, but one which does not at the present time lend itself to comparison between envelope function and exact numerical results.

The photonic crystal under study is a square lattice of vertical rods (i.e., oriented in the y direction, the axes being defined as in Fig. 1(a). The rods have a radius of $0.2a$ and the width of the waveguide is $2L = 4a$.

We compute the band structure of the bulk crystal using the MIT photonic-bands package (MPB),[17] which solves the fully vectorial Maxwell's equations with periodic boundary conditions.[18] We also use MPB to compute the modes of the 2D waveguide by taking a cross section perpendicular to the axis of the rods. Because of translational symmetry in the vertical direction, the 2D computation provides a valid means of comparison with the 3D modes calculated using the envelope function method. However, since MPB assumes periodic boundary conditions, the waveguiding structure simulated is a superlattice. Using supercells of width $32a$ was usually sufficient to prevent coupling between the parallel waveguides. A wider spacing was used for weakly guided modes.

The waveguide treatment presented above applies when the bands are well approximated by a quadratic expansion, which is the case for the two first bands. Henceforth, we focus on this portion of the band structure.

We begin by considering the case in which the average index in the core is higher than in the cladding. For the cladding material, the rods have $\epsilon = 10$ and the background medium is air. We choose a contrast $\Delta_0 = 0.1$, which means that the rods in the core have $\epsilon = 11$ and lie in a medium of $\epsilon = 1.1$. (This value being close to $\epsilon = 1$, the same background material could be used in both core and cladding in actual device designs.) Guided modes will exist where the curvature is positive, which occurs at $k_\perp = 0$ for the first two bands. Figure 3(a) shows the dispersion relation for $k_\parallel$ sweeping the entire first Brillouin zone. The shape of the modes at the edge of the Brillouin zone is shown in Figs. 3(b),3(c). The cross section of the amplitude of the electric field computed numerically with MPB was taken at an arbitrary position along the x axis. The frequency of the modes obtained using the envelope approximation method and numerical 2D computation using MPB match withing a few tenths of percent. As shown, there exists always at least one guided mode. An odd mode is added when the single-mode condition Eq. (28) ceases to be satisfied.

These results provide a numerical justification of the physical picture presented in the introduction and depicted in Fig. 1(b). As expected, the rapid variations of the electric field are features due to the crystalline structure, whereas the
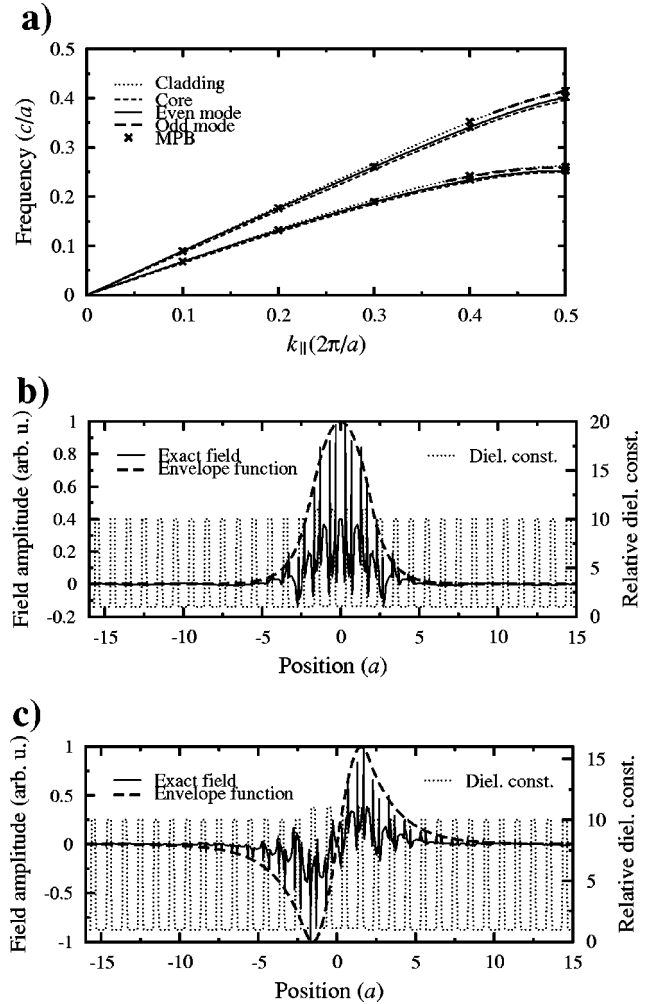

FIG. 3. Average refractive index higher in the core than in the cladding ($k_\perp = 0$). (a) Dispersion relation of the waveguide and band structure of the core and cladding materials. (b) Even and (c) odd modes of the first band for $k_\parallel = \pi/a$.

envelope behaves as though the core and cladding were continuous media.

As mentioned earlier, photonic crystal waveguiding is possible even when the average index in the core is lower than that in the cladding. We interchange the roles of the core and the cladding in the example above: the cladding material is now made of rods of $\epsilon = 11$ in a background of $\epsilon = 1.1$, while the core is made of rods having $\epsilon = 10$ lying in air. In this case, the contrast is $\Delta_0 \approx -0.091$, the cladding being the reference (unperturbed) material. Guided modes are allowed where the curvature of the bands is negative, which occurs at $k_\perp = \pi/a$ in the case of the first two bands. As seen in Eq. (14), this transverse component of the wave vector introduces a modulation to the envelope function in the transverse direction, so that the actual slowly varying envelope of the mode is the function $f_{n\mathbf{k}_0}$. This modulation explains why the envelope function and actual field have opposite parities. The dispersion relation and shapes of the modes are displayed in Fig. 4. The frequencies obtained using the envelope approximation match the exact numerical results within 1%.
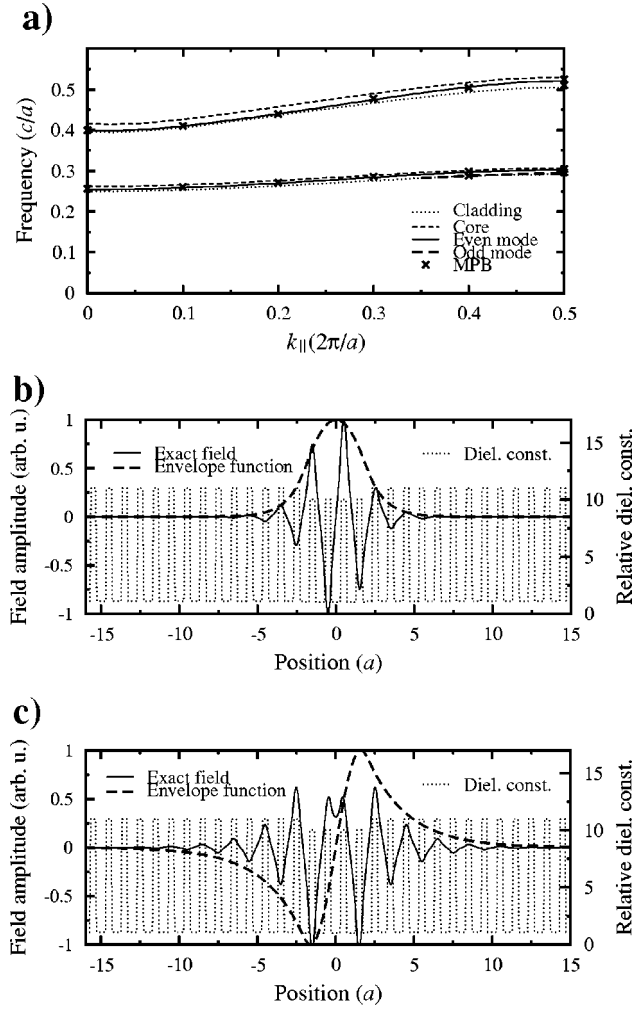
a)

b)

c)

FIG. 4. Average refractive index lower in the core than in the cladding ($k_\perp = \pi/a$). (a) Dispersion relation of the waveguide and band structure of the core and cladding materials. (b) Even and (c) odd modes of the first band for $k_\parallel = \pi/a$.

VII. CONCLUSION

We have developed an envelope approximation formalism to study 3D photonic crystal heterostructures. The power of the method lies in the fact that only knowledge of the band structure of the bulk crystal and heterostructure design are required. Thus, the bulk photonic crystal can be investigated seperately, and then employed into the calculation of the heterostructure. When applied to photonic crystal waveguides, this approach yields a direct picture of the waveguiding mechanism, allowing us to predict the frequency of the guided modes, the dispersion relations of waveguides and the shapes of the modes. The results obtained with our envelope approximation method are in excellent agreement with a fully vectorial computation of the field.

APPENDIX

This appendix provides the detailed evaluation of the rightmost term of Eq. (8) leading to Eq. (10). Taking the inner product of Eq. (8) with a mode $\mathbf{E}_{n'\mathbf{k}'}$, we must evaluate the integral

$$I \equiv \int e^{i(\mathbf{k}-\mathbf{k}')\cdot\mathbf{r}} \mathbf{u}^*_{n'\mathbf{k}'}(\mathbf{r}) \cdot \epsilon(\mathbf{r})\Delta(\mathbf{r})\mathbf{u}_{n\mathbf{k}}(\mathbf{r})d\mathbf{r}. \quad \text{(A1)}$$

The periodic function $\mathbf{u}^*_{n'\mathbf{k}'} \cdot \epsilon\mathbf{u}_{n\mathbf{k}}$ can be expanded in a Fourier series

$$\mathbf{u}^*_{n'\mathbf{k}'}(\mathbf{r}) \cdot \epsilon(\mathbf{r})\mathbf{u}_{n\mathbf{k}}(\mathbf{r}) = \sum_m b_m e^{i\mathbf{K}_m\cdot\mathbf{r}}, \quad \text{(A2)}$$

where the $\mathbf{K}_m$ are reciprocal lattice vectors. The Fourier coefficients are given by

$$b_m \equiv \frac{1}{V_0}\int_{\text{cell}} \mathbf{u}^*_{n'\mathbf{k}'}(\mathbf{r}) \cdot \epsilon(\mathbf{r})\mathbf{u}_{n\mathbf{k}}(\mathbf{r})e^{-i\mathbf{K}_m\cdot\mathbf{r}}d\mathbf{r}, \quad \text{(A3)}$$

where the integration is carried out over the volume V_0 of a unit cell. The integral (A1) becomes

$$I = \sum_m b_m \int e^{i(\mathbf{k}-\mathbf{k}'+\mathbf{K}_m)\cdot\mathbf{r}}\Delta(\mathbf{r})d\mathbf{r}$$

$$\equiv \sum_m b_m\tilde{\Delta}(\mathbf{k}-\mathbf{k}'+\mathbf{K}_m), \quad \text{(A4)}$$

where $\tilde{\Delta}(\mathbf{k})$ denotes the Fourier transform of $\Delta(\mathbf{r})$.

In order to simplify the summation, we use the fact that the length scale of the dielectric perturbation $\Delta(\mathbf{r})$ is much larger than the lattice constant, so that its Fourier components $\tilde{\Delta}(\mathbf{k})$ are negligible except for $|\mathbf{k}| \ll 1/a$. In Eq. (A4), this means that we keep only the terms for which $\mathbf{k}-\mathbf{k}' + \mathbf{K}_m \approx 0$. Now, because $\mathbf{k}$ and $\mathbf{k}'$ can always be taken in the first Brillouin zone and that $\mathbf{K}_m$ is a reciprocal lattice vector, the only way of satisfying $\mathbf{K}_m = \mathbf{k}-\mathbf{k}'$ is to take $\mathbf{K}_m = 0$, or $m = 0$. The integral becomes

$$I \approx b_0\tilde{\Delta}(\mathbf{k}-\mathbf{k}'). \quad \text{(A5)}$$

A second approximation is used to simplify the coefficient b_0. As mentioned in the text, we neglect the coupling between the bands due to the perturbation by assuming that the scalar product $\mathbf{u}^*_{n'\mathbf{k}'}(\mathbf{r}) \cdot \epsilon(\mathbf{r})\mathbf{u}_{n\mathbf{k}}(\mathbf{r})$ can be approximated by $\mathbf{u}^*_{n'\mathbf{k}}(\mathbf{r}) \cdot \epsilon(\mathbf{r})\mathbf{u}_{n\mathbf{k}}(\mathbf{r})$. Making use of the orthogonality of the Bloch functions Eq. (5),

$$b_0 \approx \frac{1}{V_0}\int_{\text{cell}} \mathbf{u}^*_{n'\mathbf{k}}(\mathbf{r}) \cdot \epsilon(\mathbf{r})\mathbf{u}_{n\mathbf{k}}(\mathbf{r})d\mathbf{r} = (2\pi)^3\delta_{n'n}. \quad \text{(A6)}$$

The integral (A5) may thus be approximated as

$$I \approx (2\pi)^3\delta_{n'n}\int \Delta(\mathbf{r})e^{i(\mathbf{k}-\mathbf{k}')\cdot\mathbf{r}}d\mathbf{r}. \quad \text{(A7)}$$

Substituting this expression into Eq. (8) and interchanging the order of integration, we get Eq. (10).

[1] Z. Zhang and S. Satpathy, Phys. Rev. Lett. **65**, 2650 (1990).

[2] M. Sigalas, C.M. Soukoulis, E.N. Economou, C.T. Chan, and K.M. Ho, Phys. Rev. B **48**, 14 121 (1993).

[3] J.B. Pendry, J. Phys.: Condens. Matter **8**, 1085 (1996).

[4] S. Kuchinsky, D.C. Allan, N.F. Borrelli, and J.-C. Cotteverte, Opt. Commun. **175**, 147 (2000).

[5] S.G. Johnson, P.R. Villeneuve, S. Fan, and J.D. Joannopoulos, Phys. Rev. B **62**, 8212 (2000).

[6] M. Lončar, T. Doll, J. Vučković, and A. Scherer, J. Lightwave Technol. **18**, 1402 (2000).

[7] A. Mekis, J.C. Chen, I. Kurland, S. Fan, P.R. Villeneuve, and J.D. Joannopoulos, Phys. Rev. Lett. **77**, 3787 (1996).

[8] S. Fan, S.G. Johnson, and J.D. Joannopoulos, J. Opt. Soc. Am. B **18**, 162 (2001).

[9] R. Stoffer, H.J.W.M. Hoekstra, R.M. de Ridder, E. van Groesen, and F.P.H. van Beckum, Opt. Quantum Electron. **32**, 947 (2000).

[10] J.C. Slater, Phys. Rev. **76**, 1592 (1949).

[11] G.H. Wannier, Phys. Rev. **52**, 191 (1935).

[12] G.F. Koster and J.C. Slater, Phys. Rev. **95**, 1167 (1954).

[13] C. Kittel and A.H. Mitchell, Phys. Rev. **96**, 1488 (1954).

[14] J.M. Luttinger and W. Kohn, Phys. Rev. **97**, 869 (1954).

[15] J.P. Albert, C. Jouanin, D. Cassagne, and D. Bertho, Phys. Rev. B **61**, 4381 (2000).

[16] J. D. Joannopoulos, R. D. Meade, and J. N. Winn, *Photonic Crystals* (Princeton University Press, Princeton, 1995).

[17] S.G. Johnson and J.D. Joannopoulos, "The MIT Photonic-bands Package," URL http://ab-initio.mit.edu/mpb/

[18] S.G. Johnson and J.D. Joannopoulos, Opt. Express **8**, 173 (2001).